

Effects of Solar Eclipse on Long Path VLF Transmission

S.S. De¹, B.K. De², B. Bandyopadhyay¹, S. Paul¹, S. Barui¹,
D.K. Haldar¹, M. Sanfui¹, T.K. Das¹, G. Chattopadhyay¹, P. Pal³

¹Centre of Advanced Study in Radio Physics and Electronics,
University of Calcutta 1, Girish Vidyaratna Lane, Kolkata 700 009, India

²Department of Physics, Tripura University, Tripura (West),
Suryamaninagar 799 130, India

³Department of Physics, M. B. B. College, Agartala 799 004, Tripura, India

Received 26 March, 2011

Abstract. The variations of phase and amplitude of a subionospheric transmitted signal at frequency 19.8 kHz from North West Cape, Australia (latitude: 21.82°S; longitude: 114.16°E) measured at Kolkata (latitude: 22.56°N, longitude: 88.5°E) during the period of solar eclipse (partial, 91.1%) on July 22, 2009 will be presented in this paper. The variations in amplitude are quite significant than the usual ambient values of the adjacent 5 days of the day of eclipse for the same period. During eclipse, the height of reflection of VLF (very low frequency) signal has been increased by 3 km. The conductivity parameter and the sharpness parameter are calculated using phase and amplitude variation of VLF signal. Plausible explanations of these changes in amplitude and phase are presented. The waveguide parameters, viz., conductivity parameter (ω_r) and sharpness parameter (β) related to VLF propagation in the Earth-ionosphere waveguide are considered to be responsible for signal attenuation.

PACS codes: 92.60.Pw, 94.20.Vv

1 Introduction

Continuous monitoring of very low frequency (VLF) signal amplitude and phase reveals the diurnal and seasonal behaviour of the lower ionosphere upon which signatures of geophysical events, *e.g.*, solar flare, sunspot activity, earthquakes, cyclones, meteor showers, polar-cap events, magnetic activity, nuclear explosions are distinctly impressed. VLF sub-ionospheric and sferics signal amplitudes are directly affected by global thunderstorm activities [1,2], solar irradiations, ionization of ionospheric constituents at lower region of the atmosphere and the conductivity of the lower ionosphere. Meteorological parameters also

have prominent influence upon the amplitude of VLF sferics, amplitude and phase of the transmitted VLF signals.

VLF electromagnetic wave from fixed station and fixed power of radiation propagates in the spherical waveguide between the Earth's surface and the lower ionosphere. It can reach several thousand kilometers away from its transmitter. Diurnal behaviours of VLF signals over long distances (> 5000 km) were first observed by Yokoyama and Tanimura [3], and diurnal phase variations by Pierce [4]. Identical experiments were also performed [5,6]. The experiments had shown a good correlation between phase and amplitude variations during sunrise and sunset transitions. Later on, VLF amplitude and phase measurements have been carried out by various investigators [7-9].

VLF radio waves are propagated in the Earth-ionosphere wave-guide delimited by the ground and the ionospheric D-region. Solar eclipses are known to produce disturbances in the lower ionosphere, which result in noticeable effects on the propagation of VLF radio waves. The changes in height of the D-region during solar eclipse are followed by phase change and amplitude variations of the VLF signal propagated through earth-ionosphere waveguide. Earlier investigators studied the effects of solar eclipse on VLF signal amplitude and their phase changes [10,11-13] along different paths of variable distance and orientation. These kinds of measurements are linked with the changes in the lower part of upper atmosphere.

On the other hand, measurements of near-earth atmospheric electricity parameters during solar eclipse give significant scopes to investigate their characteristics which are modeled by various investigators through different techniques [14,15]. Though the atmospheric electricity parameters are directly related to the global thunderstorm activities and solar radiation, there are several attempts that report the changes in the near surface electric field during solar eclipse [16,17-19]. The changes in ionospheric height and ionization jointly affect the amplitude and phase of the transmitted signal. The change in atmospheric conductivity and air-earth current may also have control over the amplitude and phase of VLF signal.

In this paper, the outcome of the simultaneous measurements of phase and amplitude variations of a VLF sub-ionospheric signal at Kolkata (latitude: 22.56° N, longitude: 88.5° E) during the period of solar eclipse on July 22, 2009, are reported. The path of the VLF signal transmitted from North West Cape, Australia (latitude: 21.82° S; longitude: 114.16° E) has been shown by the line 'TA' (Figure 1). During the maximum phase of occurrence of solar eclipse, 91% occultation was observed from Kolkata and about 65% of the propagation path of the signal at frequency 19.8 kHz transmitted from North West Cape, Australia, was under occultation.



Figure 1. The detail of the eclipse path and propagation path are depicted. **PQ** is the path of totality. The lines **EF** and **GH** represent the occurrence of 60% and 40% of the totality during maximum phase. **T** is the transmitting centre, **A** is the receiving centre and **TA** shows the propagation path.

2 Instrumentation and the Method of Observations

A copper wire of SWG value 8 and length 120 m is used as an inverted L-type antenna for receiving the vertically polarized electric field (E-field). The antenna is erected horizontally at a height of about 30 m above the ground. The signals are fed to a signal processor which is tuned at 19.8 kHz. The Q-value is maintained at 300. To ensure high selectivity, the induction coil is mounted inside a pot-core of ferrite material. The signal from the tuning stage is fed to an AC amplifier using OP AMP ICOP27 in a non-inverting mode. The AC signal at 19.8 kHz is then passed to the input of a detector circuit through a unit gain buffer. In the detector circuit, the diode OA79 is used in the negative rectifying mode. The output of the diode is obtained across a parallel combination of resistance and capacitance. The level of the detected envelope is proportional to the RMS value of the AC signal. The detected RMS output is amplified by a quasi-logarithmic dc amplifier using OP AMP 741 in the DC mode of operation. The recording time constant of RMS value is 15 sec. The calibration of the recording system has been done using a standard signal generator. During calibration, the antenna was disconnected and replaced by the standard signal

generator through a capacitance having a value equal to the terminal capacitance of the antenna. At first, the outputs are calibrated in terms RMS value of the induced voltages at the antenna. To get very low signals from the function generator, a dB-attenuator is used. The output is calibrated in terms induced voltage at the antenna in dB above $1 \mu\text{V}$. The data in the form of RMS value are recorded by digital technique using a data acquisition system. The digital data acquisition system uses a PCI 1050, 16 channel 12 bit DAS card (Dyalog). It has a 12 bit A/D converter, 16 digital input and 16 digital output. The input multiplexer has a built-in over-voltage protection arrangement. All the I/O parts are accessed by 32 bit I/O instructor, thereby increasing the data input rate. It is supported by a powerful 32-bit API, which functions for I/O processing under the Windows XP operating system.

3 Results

Continuous measurement of phase and amplitude of 19.8 kHz VLF subionospheric signal has been carried out over Kolkata (latitude: 22.56°N , longitude: 88.5°E) during the period of solar eclipse on July 22, 2009, which is transmitted from North West Cape (NWC), Australia (latitude: 21.82°S ; longitude: 114.16°E). The propagation path has been shown by the line 'TA' (Figure 1). About 91% of totality of the eclipse occurred during its maximum phase of occurrence at Kolkata. Eclipse was not found at the transmitting station at North West Cape, Australia. The detail of the totality path of the eclipse and the propagation path of 19.8 kHz sub-ionospheric transmitted VLF signal from NWC to Kolkata has been depicted in Figure 1. The totality of the eclipse moves along the curve PQ. 60% and 40% of the totality during maximum phase of the eclipse occur along the path EF and GH, respectively, towards the South. 3/4th of the total path of the signal propagated from the transmitter at NWC, Australia to Kolkata covering 0–91% obscuration towards Kolkata is shown by the line DA, out of which greater than 60% obscuration occurs about 1/4th of the propagation path over the line BA. Greater than 40% but less than 60% obscuration was observed over CB. Maximum obscuration occurred between 0 and 40% over DC. The total signal path TA is about 5665 km long from North West Cape, Australia to Kolkata.

The temporal variations of VLF subionospheric transmitted signal of 19.8 kHz on July 22, 2009 during the period of solar eclipse (continuous line) and its average value over 5 days (dotted line), *i.e.*, 3 days prior to and 2 days after the solar eclipse, adjacent to the day of occurrence solar eclipse along with standard deviations from the average value plotted as error bars are depicted in Figure 2. It starts to decrease with respect to the average value of adjacent 5 days from about 03:00 IST, then showed minimum at about 05:40 IST. It attains its almost normal value at about 09:00 IST. The level of signal during eclipse is decreased by about 2.5 dB.

Effects of Solar Eclipse on Long Path VLF Transmission

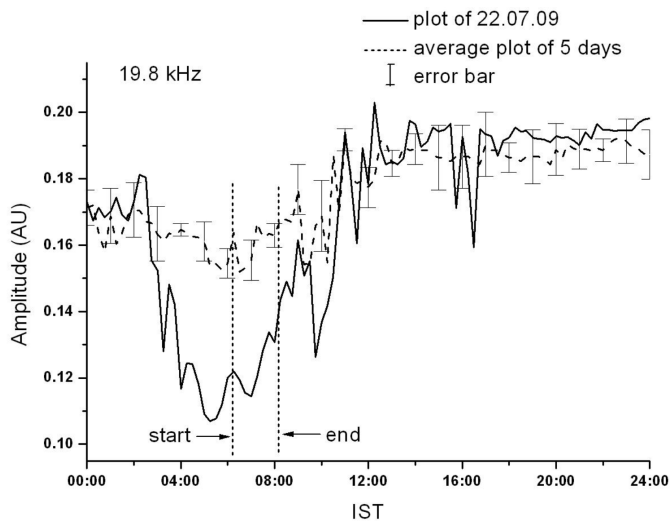


Figure 2. It depicts the amplitude variation of 19.8 kHz sub-ionspheric signal (continuous line curve) along with its averaged value for the adjacent 5 days (dotted line curve). The standard deviations from the average value are shown by error bars.

Figure 3 depicts the variations of the mean phase averaged over 5 days, *i.e.*, 3 days prior to and 2 days after the solar eclipse, adjacent to the day of occurrence of solar eclipse at every 15 minutes interval. During normal days, mean phase

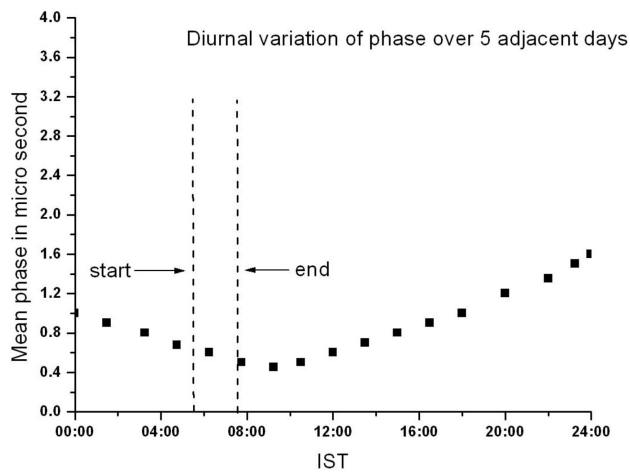


Figure 3. The variations of the mean phase averaged over 5 adjacent days of the day of occurrence of the eclipse at every 15 minutes interval are presented. 3 adjacent days prior to and 2 adjacent days after the solar eclipse.

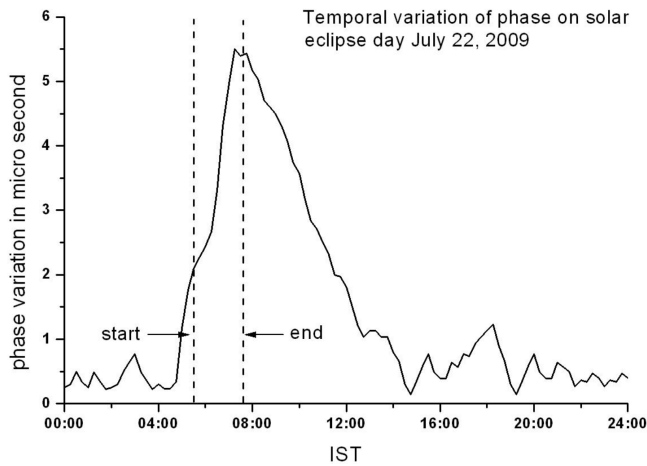


Figure 4. Retardation of phase of 19.8 kHz subionospheric signal in the propagation path as measured from Kolkata is shown.

retardation is minimum during morning hours. It shows lower values during daytime than nighttime.

Retardation of phase with time of 19.8 kHz sub-ionospheric VLF signal transmitted from North West Cape, Australia observed at Kolkata over the signal path during the day of solar eclipse is shown in Figure 4. During the solar eclipse period, *i.e.*, 05:30 IST to 07:30 IST, the ionization rate of the constituent particles at the D-region of the ionosphere decreases which causes enhancement of D-region height. As the sub-ionospheric signal is propagating through multiple reflection within the waveguide, the effective propagation path of the signal is increased which causes the observed phase delay. The phase retardation attains the maximum value of about $6 \mu\text{s}$ at 07:00 IST, although it starts to increase from 04:10 IST. The phase retardation attains its normal value as shown in the normal curve after 12:00 IST. No complete symmetry is observed in the phase variation during the eclipse period, because of uneven rate of change of ionization of the constituent particles of the D-region during the whole period of the eclipse.

4 Discussion

The waveguide formed between the lower ionosphere (D-region) and Earth's surface is good for very low frequency (VLF) propagation round the Earth. The state of the D-layer of the ionosphere is responsible to determine the amount of attenuation for VLF signal. It is also most sensitive to the loss of sunlight during solar eclipse, since it is the lowermost of the layers and is quickly overwhelmed by the neutral air around it once the active ionizing source of radiation is re-

moved. However, E layer above the D layer is more resilient to the loss of radiation and persists for a longer time. The observed phase delay in the signal asserts that the reflection height or the upper boundary of the earth-ionosphere waveguide increases. Due to lack of solar irradiation (the main source of ionization) over the eclipse zone, the ionization process at the D-region height decreases which drives the D-region height of the ionosphere upwards. As the transmitted signals propagate through the process of multiple reflections within the Earth-ionosphere waveguide, the effective propagation path of the signal increases in length which is responsible for the observed phase delay of the subionospheric transmitted signal.

The phase delay due to increase in reflection height is given in [12]:

$$\Delta\phi = 2\pi\left(\frac{d}{\lambda}\right)\left(\frac{1}{2a} + \frac{\lambda^2}{16h^3}\right)\Delta h, \quad (1)$$

where d is the distance between the transmitter and the receiver in km, λ – the wave length in km, a – the radius of the Earth, h – the normal reflecting height, Δh – the increase in reflection height.

If Δt is the time delay, then $\Delta\phi = 2\pi(\Delta t/T)$. This will be used in equation (1).

$$\therefore \frac{\Delta t}{T} = \left(\frac{d}{\lambda}\right)\left(\frac{1}{2a} + \frac{\lambda^2}{16h^3}\right)\Delta h. \quad (2)$$

Using the experimental value of Δt as observed in the case of 19.8 kHz transmitted signal and taking $h = 72$ km [7], it is found from equation (2) that $\Delta h \cong 3$ km. The waveguide formed between the lower ionosphere and Earth's surface is good for very low frequency (VLF) propagation round the Earth. The conductivity parameter determining the status of the ionospheric radio propagation is controlled by the solar conditions.

The attenuation factor (α_M) for M^{th} mode is given by [20]:

$$\alpha_M = -8.68\left(\frac{2\pi}{\lambda}\right)\text{Im}(S_M) \text{ dB km}^{-1}, \quad (3)$$

where $S_M = (1 - C_M^2)^{1/2}$, C_M being root of the modal equation given by

$$R_i \exp(ik_0 H C_M) = \exp(-i2\pi M), \quad (4)$$

where H is the height of the boundary of the ionosphere.

The Fresnel's reflection coefficient R_i of the lower boundary of the ionosphere involved in equation [20] is given by

$$R_i = \frac{\left(1 - \frac{\omega_r}{\omega}\right)^2 C_M - \left\{\left(1 - i\frac{\omega_r}{\omega}\right)^2 - S_M^2\right\}^{1/2}}{\left(1 - i\frac{\omega_r}{\omega}\right)^2 C_M - \left\{\left(1 - i\frac{\omega_r}{\omega}\right)^2 - S_M^2\right\}^{1/2}}, \quad (5)$$

where $\omega_r = \omega_0^2/\nu$ is the conductivity parameter, ω_0 is the angular plasma frequency, and ν is the collision frequency.

The conductivity parameter mentioned in the waveguide mode theory [21], is assumed to be

$$\omega_r = 2.5 \times 10^5 \exp\{\beta(h - H')\}, \quad (6)$$

where H' is the height at which $\omega_r = 2.5 \times 10^5 \text{ s}^{-1}$, β is called sharpness parameter.

For normal ionosphere $\beta = 0.43 \text{ km}^{-1}$ and $H' = 72 \text{ km}$ [7]. The present observation shows that during solar eclipse H' is increased to $72 + 3 = 75 \text{ km}$. The value of β also changes during solar eclipse [10]. The parameters β and H' jointly determine the attenuation factor. In the shadow region, variation of electron density above 80 km is negligible [22]. The variation of electron density mainly occurs between 70 and 80 km.

Using equations (4) and (5) in equation (3), the variation of attenuation factor α (in dB per 1000 km, for the first mode, $M = 1$) with ω_r is obtained. This variation for the first mode which is dominating in the case of long distance propagation is shown in Figure 5 at frequency of 19.8 kHz following the calculation of Yamashita [20]. The value of attenuation corresponding to normal value of $2.5 \times 10^5 \text{ s}^{-1}$ of ω_r is 1.76 dB per 1000 km. Since from the observation of phase delay it is confirmed that reflection height of the VLF signal has increased, according to equation (6), it is confirmed that the signal got reflected from the height at which ω_r is higher than the normal value. The present observation shows that the attenuation has increased by 2.5 dB over a path of 5665 km

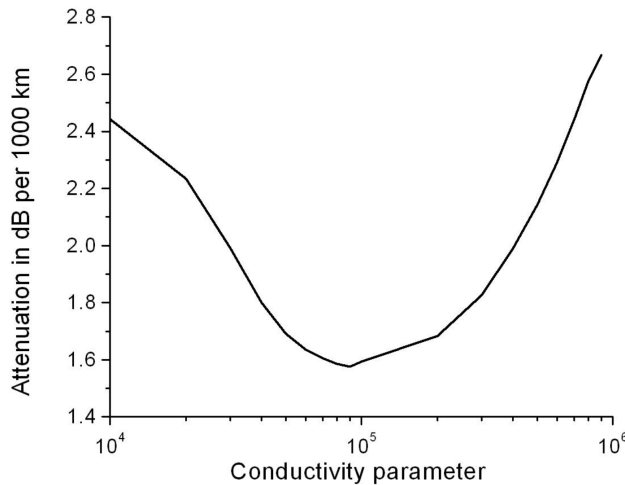


Figure 5. Variation of attenuation (in dB per 1000 km) with conductivity parameter according to waveguide mode theory at 19.8 kHz.

which comes to be an additional attenuation of 0.44 dB per 1000 km. The total observed attenuation then becomes to be $(1.76 + 0.44) = 2.2$ dB per 1000 km. From Figure 5, this attenuation corresponds to $\omega_r = 5.4 \times 10^5 \text{ s}^{-1}$. Considering the observed variation of height of reflection and the new value of conductivity parameter ω_r , the value of sharpness parameter b is found to be 0.26 km^{-1} . It asserts that during the eclipse, the sharpness of the ionosphere, *i.e.*, height gradient of electron density in the D-region is lost.

It is also to be mentioned that the formation of shadow in the ionospheric D-region gives rise to transfer of energy from the first mode to the second mode. This is due to the discontinuities raised around the shadow region. In this case, interference of first and second modes can make the resultant amplitude smaller than the normal value [23].

The atmospheric temperature drops by 2.2°C and the relative humidity increased by 2.4% during the eclipse. The variation of air-temperature, electric field, current density and conductivity over the surface of the Earth at tropical latitudes ($\pm 25^\circ$) and temperate latitudes ($\pm 60^\circ$) are interrelated with the solar radiations, global thunderstorm and lightning activity. The vast potential difference between the Earth and the ionosphere drives the air-earth current downwards from the lower region of the ionosphere to the surface of the Earth. In the absence of solar radiation during eclipse, the air-earth current may have some indirect effect on the ionization and recombination processes.

5 Conclusion

Properties of the ionospheric D-region under conditions of a solar total eclipse were measured utilizing a VLF receiving system previously by many investigators [10]. All involved path < 2000 km and $> 10\,000$ km. There is no report about path length around 5000 km. In the case of path < 2000 km, both attenuation and enhancements in amplitude are reported during solar eclipse. In the case of path $> 10\,000$ km, the increase in attenuation is reported. The present observation of increase in attenuation is similar to the propagation over long distance. In this respect we conclude that with the reduction of solar radiation, the ionization level in the range of 70-80 km in the D-region decreases. The reflection height increases to that extent where, though conductivity parameter increases, the sharpness parameter decreases appreciably from the normal value of 0.43 to 0.26 km^{-1} . The decrease in sharpness parameter causes reduction in power of the beam reflected by the ionosphere. However, the overall effect is dependent not only on the path length but also on the time of occurrence of the eclipse in a day and also in a season and frequency of observation.

Acknowledgements

The authors acknowledge with thanks the financial support from Indian Space Research Organization (ISRO) through S. K. Mitra Centre for Research in Space Environment, University of Calcutta, Kolkata, India, for carrying out the study.

References

- [1] A.P. Nickolaenko (1997) *J. Atmos. Sol. Terr. Phys.* **59** 805.
- [2] M.J. Rycroft, M. Cho (1998) *J. Atmos. Sol. Terr. Phys.* **60** 889.
- [3] E. Yokoyama, I. Tanimura (1933) *Proc. IRE* **21** 263.
- [4] J.A. Pierce (1955) *Proc. IRE* **43** 584.
- [5] D.D. Crombie, A.H. Allan, M. Newman (1958) *Proc. IRE* **105** 301.
- [6] D.D. Crombie (1964) *J. Res. Nat. Bur. Stand.* **68D** 27.
- [7] N.R. Thomson (1993) *J. Atmos. Terr. Phys.* **55** 173.
- [8] W.M. McRae, N.R. Thomson (2000) *J. Atmos. Sol. Terr. Phys.* **62** 609.
- [9] V. Zigman, D. Grubor, D. Sulic (2007) *J. Atmos. Sol. Terr. Phys.* **69** 775.
- [10] M.A. Clilverd, C.J. Rodger, N.R. Thomson, J. Lichtenberger, P. Steinbach, P. Cannon, M.J. Angling (2001) *Radio Science* **36** 773.
- [11] P. Kaufmann, R.F. Schaal (1968) *J. Atmos. Sol. Terr. Phys.* **30** 469.
- [12] P. Pant, H.S. Mahra (1994) *Indian J. Radio Space Phys.* **23** 399.
- [13] P.S. Dixit, P.K. Rao, R.V. Bhonsle, G. Sethia, M.R. Deshpande, H. Chandra (1980) *Bult. Astro. Soc. India* **8** 145.
- [14] D. Founda, D. Melas, S. Lykoudis, I. Lisaridis, E. Gerasopoulos, G. Kouvarakis, M. Petrakis, C. Zerefos (2007) *Atmos. Chem. Phys.* **7** 5543.
- [15] W. Zeng, X. Zhang, Z. Huang (1997) *Terrestrial, Atmospheric and Oceanic Sciences* **8** 233.
- [16] H. Dolezalek (1972) *Arch. Meteorol. Geophys. Bicol.* **21A** 221.
- [17] H. Dolezalek (1972) *Pure Appl. Geophys.* **100** 8.
- [18] A.K. Kamra, J.K.S. Teotia, A.B. Sathe (1982) *J. Geophys. Res.* **87** 2057.
- [19] S. Dhanorkar, C.G. Deshpande, A.K. Kamra (1989) *J. Atmos. Sol.-Terr. Phys.* **51** 1031.
- [20] M. Yamashita (1969) *J. Atmos. Terr. Phys.* **31** 1049.
- [21] J.R. Wait, K.P. Spice (1964) *NBS Tech. Note* **300**.
- [22] P.T. Verronen, E. Eulich, E. Turunem, C.J. Rodger (2006) *Ann. Geophysicae* **24** 187.
- [23] K.J.W. Lynn (1973) *J. Atmos. Terr. Phys.* **35** 439.